



## Separation Science and Engineering

Gas separation using sol-gel derived microporous zirconia membranes with high hydrothermal stability<sup>☆</sup>

Li Li, Hong Qi \*

*Membrane Science and Technology Research Center, State Key Laboratory of Materials-Oriented Chemical Engineering, Nanjing Tech University, Nanjing 210009, China*

## ARTICLE INFO

## Article history:

Received 28 January 2014

Received in revised form 26 September 2014

Accepted 23 October 2014

Available online 15 May 2015

## Keywords:

Microporous membrane

Zirconia

Gas separation

Sol-gel process

Hydrothermal stability

## ABSTRACT

A microporous zirconia membrane with hydrogen permeance about  $5 \times 10^{-8} \text{ mol} \cdot \text{m}^{-2} \cdot \text{s}^{-1} \cdot \text{Pa}^{-1}$ ,  $\text{H}_2/\text{CO}_2$  permselectivity of ca. 14, and excellent hydrothermal stability under steam pressure of 100 kPa was fabricated via polymeric sol-gel process. The effect of calcination temperature on single gas permeance of sol-gel derived zirconia membranes was investigated. Zirconia membranes calcined at 350 °C and 400 °C showed similar single gas permeance, with permselectivities of hydrogen towards other gases, such as oxygen, nitrogen, methane, and sulfur hexafluoride, around Knudsen values. A much lower  $\text{CO}_2$  permeance ( $3.7 \times 10^{-9} \text{ mol} \cdot \text{m}^{-2} \cdot \text{s}^{-1} \cdot \text{Pa}^{-1}$ ) was observed due to the interaction between  $\text{CO}_2$  molecules and pore wall of membrane. Higher calcination temperature, 500 °C, led to the formation of mesoporous structure and, hence, the membrane lost its molecular sieving property towards hydrogen and carbon dioxide. The stability of zirconia membrane in the presence of hot steam was also investigated. Exposed to 100 kPa steam for 400 h, the membrane performance kept unchanged in comparison with freshly prepared one, with hydrogen and carbon dioxide permeances of  $4.7 \times 10^{-8}$  and  $\sim 3 \times 10^{-9} \text{ mol} \cdot \text{m}^{-2} \cdot \text{s}^{-1} \cdot \text{Pa}^{-1}$ , respectively. Both  $\text{H}_2$  and  $\text{CO}_2$  permeances of the zirconia membrane decreased with exposure time to 100 kPa steam. With a total exposure time of 1250 h, the membrane presented hydrogen permeance of  $2.4 \times 10^{-8} \text{ mol} \cdot \text{m}^{-2} \cdot \text{s}^{-1} \cdot \text{Pa}^{-1}$  and  $\text{H}_2/\text{CO}_2$  permselectivity of 28, indicating that the membrane retains its microporous structure.

© 2015 The Chemical Industry and Engineering Society of China, and Chemical Industry Press. All rights reserved.

## 1. Introduction

Due to their thermal, mechanical, and chemical stability [1,2], porous ceramic membranes are the most suitable membrane materials for implementation in many petro-chemical industrial processes where harsh environment, such as high temperature and high pressure, is often encountered. Microporous ceramic membrane-based gas separation offers an environment-friendly alternative to conventional separation technologies owing to its high energy efficiency and high performance (flux and selectivity) at elevated temperatures [1,3]. Because of its inherent microstructure [4], silica-based microporous membrane is one of the most promising molecular sieving materials in view of its excellent separation performance towards small gaseous molecules such as  $\text{H}_2$ ,  $\text{N}_2$ ,  $\text{O}_2$ , and  $\text{CH}_4$ . This membrane has drawn a great deal of attentions for separation of industrial gas streams in comparison with organic

counterpart. However, it lacks microstructure stability in the presence of water at a temperature as low as 60 °C, restricting its industrial applications in gas separation such as steam-reforming of hydrocarbons and water-gas shift reaction [5]. Humidity can induce the densification of microporous silica network by the breakage of siloxane bonding in the presence of steam, followed by generation of silanol groups and subsequent recombination and rearrangement of them into the siloxane network [6]. Several approaches have been proposed for improving hydrothermal stability of silica membranes [7–9]. Firstly, metal or transition metal ions are chosen as dopants to modify the amorphous silica matrix. For example, Igi *et al.* [7] found that doping cobalt hampered the thermally induced molecular motion of silica matrix and, thereby, increased the hydrothermal stability of silica membrane. Secondly, organic functional groups were introduced into silica networks [10–13]. Duke *et al.* [11,12] reported an improved stability of carbonized silica membranes due to the remained carbon in the silica matrix, which reduces free motion of silanol groups. De Vos *et al.* [13] and Wei *et al.* [10] also dispersed organic functional groups into the silica matrix so as to make membrane structures more hydrophobic. Another strategy to overcome the instability of silica membrane in the presence of steam is to substitute tetraethylorthosilicate with other precursors, which are more hydrothermally stable, such as transition-metal alkoxides or bridged bis-silyl precursors. For example, Kanezashi *et al.* [14] fabricated a hybrid silica membrane by using 1,2-bis(triethoxysilyl)ethane

\* Supported by the National Natural Science Foundation of China (21276123, 21490581), the National High Technology Research and Development Program of China (2012AA03A606), State Key Laboratory of Materials-Oriented Chemical Engineering (ZK201002), the Natural Science Research Plan of Jiangsu Universities (11KJB530006), the "Summit of the Six Top Talents" Program of Jiangsu Province and a Project Funded by the Priority Academic Program development of Jiangsu Higher Education Institutions (PAPD).

<sup>†</sup> Corresponding author.

E-mail address: [hqjinjut@aliyun.com](mailto:hqjinjut@aliyun.com) (H. Qi).

(BTESE) as a precursor, with the membrane remaining stable in 3 kPa steam for 90 h. Nevertheless, imparting excellent hydrothermal stability to microporous membranes while retaining their flux and selectivity properties remains one of the challenges in membrane research field.

Other oxide materials such as titania, zirconia and Ti/Zr composite membranes are considered more stable in the presence of hot steam and promising for gas separation [5]. However, their permselectivities to gases with relatively small kinetic diameters, such as H<sub>2</sub>, CO<sub>2</sub>, O<sub>2</sub>, N<sub>2</sub> and CH<sub>4</sub>, are generally in the range of Knudsen values. For example, Shibao *et al.* [15] and Gu *et al.* [16] fabricated zirconia-based gas separation membranes, with permeance to H<sub>2</sub> as high as  $5 \times 10^{-6} \text{ mol} \cdot \text{m}^{-2} \cdot \text{s}^{-1} \cdot \text{Pa}^{-1}$  at the expense of low permselectivity (5–6) to H<sub>2</sub>/CO<sub>2</sub>, which is slightly higher than the Knudsen value (4.7). Coterillo *et al.* [17] reported a much lower ideal separation factor (<3) of He/CO<sub>2</sub> for a tubular ZrO<sub>2</sub> membrane calcined at 400 °C. Kreiter *et al.* [18] obtained similar results with titania microporous membranes. One of the main obstacles in such investigations is that either mesoporous membranes (with pore size larger than 2 nm) or nearly dense structures are obtained for the fabrication of titania, zirconia or Ti/Zr composite gas separation membranes. It is very difficult to quantitatively tune the pore size of oxide-based membranes in the range of 0.3–0.5 nm, which is suitable for the separation of gases with relatively small sizes, such as hydrogen and carbon dioxide.

Inspired by the results in our previous study [19], in view of zirconia as a common catalyst with acidic properties [18,20], our motivation in this research is to tune the pore size and surface acidity of zirconia membrane for the separation of H<sub>2</sub>/CO<sub>2</sub> under hydrothermal condition. In this study, we report the single gas permeance of microporous zirconia membranes and examine the hydrothermal stability of a sol–gel derived microporous zirconia membrane in the presence of 100 kPa steam.

## 2. Experimental

### 2.1. Sol synthesis

Zirconia polymeric sol was synthesized by using zirconium *n*-propoxide (70% in propanol, ABCR GmbH, denoted as ZnP) as a precursor and diethanolamine (DEA) as a chelating agent. 4.5 ml of ZnP was added to 20 ml of 1-propanol, and then 2.1 ml of DEA was drop-wise introduced into the ZnP solution with vigorous stirring. Both operations were carried out in a nitrogen glove box. The mixture was immediately placed in an ice bath to prevent premature hydrolysis. 0.9 ml of deionized water was drop-wise added into the above-mentioned solution with vigorous stirring and subsequently maintained at 273 K for hydrolysis and condensation for 12 min. The obtained zirconia polymeric sol had a final molar ratio of 1:28.9:2.2:5 (ZnP:1-propanol:DEA:H<sub>2</sub>O) and was diluted 6 times with 1-propanol before dip-coating.

### 2.2. Preparation of powder and membrane

Supported microporous zirconia membranes were fabricated through a single dip-coating of zirconia sol onto home-made disk  $\alpha$ -alumina supported mesoporous  $\gamma$ -alumina layers under clean room (class 1000) conditions. The gamma alumina layer was calcined at 550 °C with the final pore size of 4–5 nm. Dip-coating was performed at a velocity of 12 mm·s<sup>-1</sup> by using a MEMDIP 5 coating device (Pervatech B. V., The Netherlands). Then zirconia membranes were calcined in the air at 350 °C, 400 °C and 500 °C for 3 h (referred to as Zr-350, Zr-400, and Zr-500, respectively), with both heating and cooling rates of 0.5 °C·min<sup>-1</sup>. Zirconia powder was obtained by drying corresponding zirconia polymeric sols in a Petri dish at 100 °C, followed by calcination procedure the same as that for supported zirconia membranes.

### 2.3. Characterization

Effective particle size in the zirconia polymeric sol was measured by using a Zetatracer analyzer (Microtrac Inc.), based on the dynamic light scattering and Mie scattering theory. The particle size distribution of polymeric zirconia sols was derived from a cumulant analysis in the Microtrac software. Thermal evolution of dried zirconia powder was determined using a combined thermogravimetry and differential thermal analysis (TG-DTA) apparatus (STA-449-F3, Netzsch), under air atmosphere (flow rate: 30 ml·min<sup>-1</sup>) with a heating rate of 10 °C·min<sup>-1</sup> in the temperature range of 40–1000 °C. Phase composition of zirconia powder heat-treated at different temperatures and with steam treatment was evaluated by employing X-ray diffraction (XRD, Bruker D8, Advance diffractometer), using a target of Cu K $\alpha$  operated at 40 kV and 40 mA. Nitrogen adsorption measurements were conducted at 77 K (N<sub>2</sub>) on BELSORP-mini instrument (BEL Inc.). Prior to measurements, all samples were degassed at 200 °C for 3 h under vacuum. Temperature-programmed desorption of ammonia (NH<sub>3</sub>-TPD, TP5080, Xianquan Co. Ltd, Tianjin, China) was used to evaluate the acidity of zirconia powder before and after steam treatment.

Single gas permeation measurements of zirconia membranes were conducted in a dead-end mode set-up. The membranes were sealed in a stainless steel module using fluoroelastomer O-rings with the separation layer exposed to the feed side. The pressure difference across the membrane and the cell temperature were set at 0.3 MPa and 200 °C, respectively, while the permeate side was vented to the atmosphere. Single gas permeances of zirconia membranes were measured in sequence, starting with the smallest kinetic diameter, from H<sub>2</sub> (0.289 nm), CO<sub>2</sub> (0.33 nm), O<sub>2</sub> (0.346 nm), N<sub>2</sub> (0.365 nm), CH<sub>4</sub> (0.382 nm) to SF<sub>6</sub> (0.55 nm). The permselectivity, also known as ideal selectivity, was calculated based on ratios between permeance values for pure gases throughout the study. Hydrothermal stability of a membrane was tested by measuring its single gas permeance at 200 °C, before and after in-situ exposure to steam at 100 kPa over a total period of 1250 h. The temperature for exposure of membrane to steam was 200 °C. Further stability tests were carried out by putting zirconia powder in saturated steam at 200 °C (corresponding to a pressure of 1550 kPa) in an autoclave for 100 and 300 h. Nitrogen adsorption measurements, XRD and NH<sub>3</sub>-TPD characterizations were conducted on samples and compared with that of zirconia powder without steam treatment, so as to evaluate their hydrothermal stability.

## 3. Results and Discussion

### 3.1. Properties of zirconia polymeric sols

Fig. 1 shows the particle size distributions of zirconia polymeric sols immediately after synthesis and stored at –20 °C for various time intervals. The particle size of freshly prepared zirconia sol was in the range of 1.5–15 nm, with an average value of 3.3 nm. When stored at –20 °C for 1 month and 2 months, the particle size distribution shifted slightly, with the average particle size being 3.7 and 3.9 nm, respectively. With storage at –20 °C for over 3 months the particle size increased slightly to an average value of 4.6 nm. However, the maximum particle size did not vary much during the storage. The sol kept clear and transparent after storage at –20 °C over 3 months. The results confirm a high sol stability and suitable particle size distribution as required for practical deposition of the sol onto a mesoporous substrate.

### 3.2. Thermal evolution of sol–gel derived zirconia powder

Fig. 2 shows thermogravimetric (TG) and differential thermal analysis (DTA) data of dried zirconia powder. Four exothermic peaks are apparent, corresponding to temperatures 347.5 °C, 387.5 °C, 492.5 °C and 682.5 °C. The initial mass loss up to temperature of 250 °C is due to the removal of physically absorbed water and solvent. The exothermic

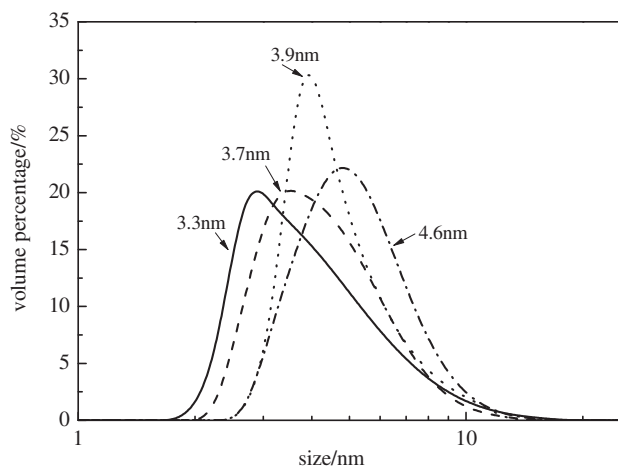


**Fig. 1.** Particle size distribution of freshly prepared zirconia polymeric sol and its stability at storage temperature of  $-20^{\circ}\text{C}$ . — freshly prepared; --- after storage for 1 month; .... after storage for 2 months; -·- after storage for 3 months.

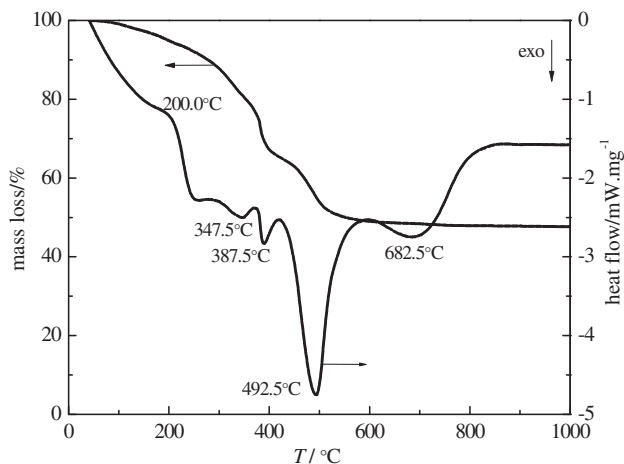


**Fig. 2.** TG-DTA curves of zirconia powder measured under oxygen atmosphere.

peak with 10.9% mass loss at  $347.5^{\circ}\text{C}$  is attributed to the removal of ligands inside the zirconia powder [4]. Because the reported phase transition temperature from amorphous to tetragonal zirconia is in the range of  $400\text{--}500^{\circ}\text{C}$  [21–23], the exothermic peak at  $387.5^{\circ}\text{C}$  can be assigned to the decomposition of organic functional groups or charring [21,22]. A large exothermic peak can be observed at  $492.5^{\circ}\text{C}$ , with a sharp decrease in mass of approximately 16.2%. This may be attributed to the removal of chelated zirconium complex inside the zirconia powder [24]. The exothermic peak at  $682.5^{\circ}\text{C}$ , without any mass loss, can be ascribed to the phase transformation from tetragonal zirconia to monoclinic zirconia, as reported by Agoudjil *et al.* [25]. This result is consistent with the observations by XRD.

Fig. 3 gives XRD patterns of zirconia powder dried at  $100^{\circ}\text{C}$  and thermally treated in the temperature range of  $200\text{--}700^{\circ}\text{C}$ . The absence of any Bragg reflections in the zirconia powder heat-treated at temperatures up to  $350^{\circ}\text{C}$  indicates the formation of amorphous phases. A weak diffraction peak was observed at  $30.3^{\circ}$  ( $2\theta$ ) for Zr-400 powder. For the powder calcined at higher than  $400^{\circ}\text{C}$ , more Bragg reflections, at  $2\theta = 30.3^{\circ}, 35.0^{\circ}, 50.2^{\circ}$  and  $63.0^{\circ}$ , are apparent, corresponding to the characteristic peaks of tetragonal zirconia phases. The results are consistent with that reported in references [20,26,27]. It should be noted that  $700^{\circ}\text{C}$ -calcined powder shows not only the tetragonal phase, but also the peaks at  $2\theta = 28.3^{\circ}$  and  $31.4^{\circ}$  (corresponding to monoclinic zirconia). Both the heating and cooling rates for calcination

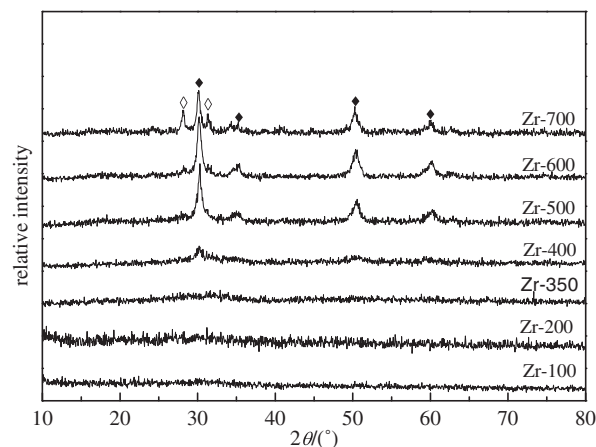


**Fig. 3.** XRD patterns of zirconia powder heat-treated at various temperatures. ◆ tetragonal; ◇ monoclinic.

of the powder are  $0.5^{\circ}\text{C}\cdot\text{min}^{-1}$ , while the heating rate for TG-DTA test is  $10^{\circ}\text{C}\cdot\text{min}^{-1}$ . Because of the large difference in the ramping rate, the crystallization transition temperature of powder will shift to lower temperature as depicted in XRD patterns. There is a volume increase during phase transition from tetragonal to monoclinic zirconia, which should be avoided in view of the membrane integrity. In addition, amorphous phases in the membrane are apt to maintain its microporous structure, while the membrane with crystalline structure will endure harsh environment better. Thus a trade-off must be considered to fabricate microporous membranes. The crystallization of zirconia may lead to grain growth and increase the pore size to mesoporous domain, so that the calcination temperature should be accurately controlled.

In order to study the effect of calcination temperature on pore structures, nitrogen sorption measurements were carried out on zirconia powder calcined at  $350^{\circ}\text{C}$ ,  $400^{\circ}\text{C}$  and  $500^{\circ}\text{C}$ , with the results displayed in Fig. 4. The sorption data of Zr-350 powder is in coincidence with type I isotherm, though the adsorption and desorption curves does not overlap. It is reported that type I isotherms are given by microporous solids with relatively small external surfaces, with the limiting uptake governed by accessible micropore volume rather than by internal surface area [28]. However, the much lower adsorption amount indicates a small fraction of micropores in Zr-350 powder. A steep rise in the adsorption curve of Zr-400 powder at the relative pressure ( $p/p_0$ ) of  $0\text{--}0.1$  and more nitrogen adsorption amount demonstrates the increase of micropores. A hysteresis loop associated with the capillary condensation in mesopores and the

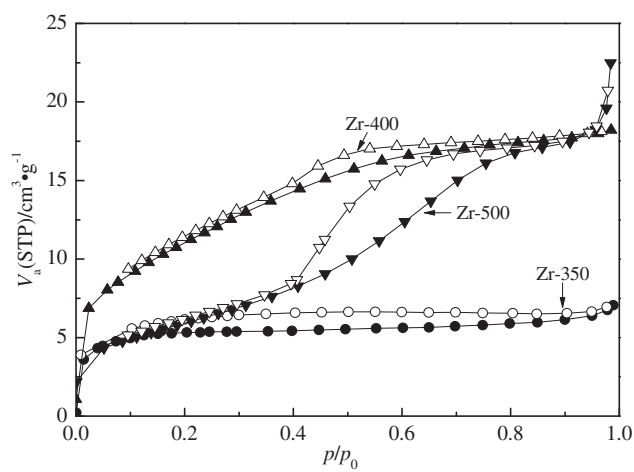


**Fig. 4.** Nitrogen adsorption/desorption isothermal curves of  $\text{ZrO}_2$  powder heat-treated at various temperatures.

limiting uptake for  $p/p_0 > 0.5$  are obtained in Zr-400 sorption curves, indicating that 400 °C-calcined powder consists of both micropores and mesopores. For the zirconia powder thermally treated at 500 °C, a distinct hysteresis loop can be detected, which is the characteristic of type IV isotherm, indicating the formation of more mesopores. However, an obvious uptake over a range of high  $p/p_0$  ( $>0.9$ ) indicates the presence of macropores in Zr-500 powder at elevated calcination temperature. The results can be confirmed quantitatively by micropore volume ( $V_{mi}$ ) and total volume ( $V_T$ ), calculated by adsorption capacities at relative pressures of 0.1 and 0.95. The mesopore volume ( $V_{me}$ ) is obtained by subtracting  $V_{mi}$  from  $V_T$  [29]. The  $V_{mi}/V_T$  values of Zr-350, Zr-400 and Zr-500 powder are 0.778, 0.513 and 0.276, respectively, displayed in Table 1. The microporous and total volumes are obtained by recording the adsorbed volume of powder at  $p/p_0 = 0.1$  and  $p/p_0 = 0.95$  [29]. The  $V_{mi}/V_T$  ratio of zirconia powder decreases with the increase of calcination temperature, from 0.778 (350 °C) to 0.276 (500 °C), so that the increase of calcination temperature results in the transformation of powder from a majority of microporous structure to a minority one. Large pores form at higher calcined temperature.

### 3.3. Single gas permeability of microporous $ZrO_2$ membranes

Fig. 5 shows single gas permeance of microporous zirconia membranes calcined at 350 °C, 400 °C and 500 °C. Unfortunately, molecular sieving effect is not found, so that the ideal selectivity of the membrane is mostly around Knudsen values. The hydrogen permeance of Zr-350 membrane is  $5.3 \times 10^{-8} \text{ mol} \cdot \text{m}^{-2} \cdot \text{s}^{-1} \cdot \text{Pa}^{-1}$ , while those for oxygen, nitrogen, methane and sulfur hexafluoride are  $1.5 \times 10^{-8}$ ,  $1.7 \times 10^{-8}$ ,  $1.9 \times 10^{-8}$  and  $7.4 \times 10^{-9} \text{ mol} \cdot \text{m}^{-2} \cdot \text{s}^{-1} \cdot \text{Pa}^{-1}$ , respectively, corresponding to ideal selectivities of 3.5 ( $H_2/O_2$ ), 3.1 ( $H_2/N_2$ ), 2.8 ( $H_2/CH_4$ ) and 7.2 ( $H_2/SF_6$ ). It should be noted that the transportation of carbon dioxide across the zirconia membrane exhibits much lower permeance of  $3.7 \times 10^{-9} \text{ mol} \cdot \text{m}^{-2} \cdot \text{s}^{-1} \cdot \text{Pa}^{-1}$ . The ideal selectivity of Zr-350 membrane with respect to  $H_2/CO_2$  is 14.3, which is much higher than that of Knudsen value (4.7). Although Zr-350 and Zr-400 powders exhibit quite different performance (Figs. 3 and 4), the hydrogen permeance ( $\text{ca. } 5 \times 10^{-8} \text{ mol} \cdot \text{m}^{-2} \cdot \text{s}^{-1} \cdot \text{Pa}^{-1}$ ) of Zr-400 membrane is almost the same as that of Zr-350 membrane. Thus the permselectivity of  $H_2/CO_2$  for Zr-400 membrane retains at a relatively high value, while the transportation of other gases follows the Knudsen mechanism. For Zr-500 membrane, the single gas permeance is much higher,  $4.37 \times 10^{-7}$  and  $7.1 \times 10^{-8} \text{ mol} \cdot \text{m}^{-2} \cdot \text{s}^{-1} \cdot \text{Pa}^{-1}$  to hydrogen and SF<sub>6</sub>, respectively, which are one order of magnitude higher than that of Zr-350 and Zr-400 membranes. The ideal selectivities of Zr-500 membrane for  $H_2/O_2$ ,  $H_2/N_2$ , etc. are all around Knudsen values, including  $H_2/CO_2$ . From the X-ray diffraction and nitrogen sorption data of 500 °C-calcined zirconia powder as shown in Figs. 3 and 4, single gas permeance of Zr-500 membrane is reasonable since the performance of powder is in conformity with corresponding mesoporous materials. The TG analysis (Fig. 2) clearly shows that the weight loss is completed at around 500 °C, and the membranes calcined at 350 °C and 400 °C exhibit the highest  $H_2/CO_2$  permselectivity. Residual carbonaceous species may still be present in the separation layer. We have proposed that doping of transition metal into the microporous siliceous networks generates Lewis acid

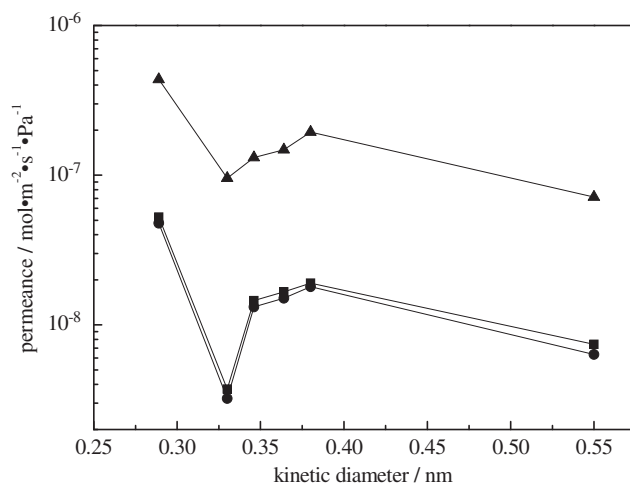


Fig. 5. Single gas permeance of microporous zirconia membranes (calcined at 350 °C, 400 °C and 500 °C) as a function of kinetic diameter of permeating gas molecule (200 °C and 0.3 MPa). ■ Zr-350; ● Zr-400; ▲ Zr-500.

on the membrane surface and, eventually, impart sufficient high  $H_2/CO_2$  permselectivity to Nb-BTESE derived microporous membranes. That is, the presence of acid sites on membrane surface may play an important role in the reduction of  $CO_2$  permeance. To confirm the presence of acidic sites on the zirconia membrane surface, the TPD test for zirconia powder calcined at different temperatures was carried out by using NH<sub>3</sub> molecule as a probe, with the data displayed in Fig. 6. All ZrO<sub>2</sub> powders show similar profiles with two desorption signals in temperature range of 70–133 °C and 470–475 °C, indicating that both weak and medium strong acid sites are generated in zirconia powder. The results are consistent with the data in references [30–33]. It should be noted that

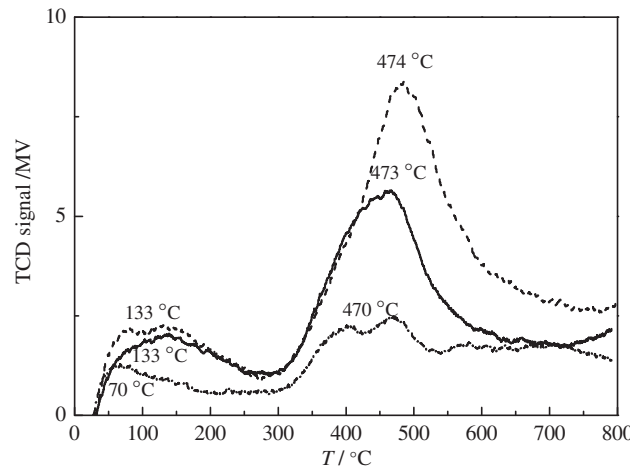


Fig. 6. NH<sub>3</sub>-TPD curves of ZrO<sub>2</sub> powder heat-treated at various temperatures. — Zr-350; - - Zr-400; - · - Zr-500.

Table 1  
Properties of ZrO<sub>2</sub> powder thermally treated at various temperatures

Thermally treated temperature/°C	BET specific surface area/ $\text{m}^2 \cdot \text{g}^{-1}$	Average pore diameter/nm	$V_{mi}/\text{cm}^3 \cdot \text{g}^{-1}$	$V_T/\text{cm}^3 \cdot \text{g}^{-1}$	$V_{mi}/V_T$
100	0.52	4.62	0.000109	0.000583	0.187
200	1.53	6.48	0.000447	0.002127	0.210
350	8.82	4.95	0.007689	0.009887	0.778
400	29.91	3.77	0.014276	0.027824	0.513
500	21.74	6.40	0.007788	0.028187	0.276
600	7.23	14.54	0.003179	0.020415	0.158
700	3.71	26.13	0.001816	0.018613	0.098

Note:  $V_{mi}$  and  $V_T$  are expressed as liquid volumes; STP: standard temperature and pressure.

the acidic properties of Zr-350 powder are roughly the same as those of Zr-400 powder. However, in comparison with zirconia powders heat-treated at 350 °C and 400 °C, the acidic property of Zr-500 powder is much weaker, as evidenced by the lower amplitude and shift of desorption peaks towards lower temperatures. The results demonstrate that much higher H<sub>2</sub>/CO<sub>2</sub> permselectivity may be obtained with Zr-350 and Zr-400 membranes by their microporous structures. However, the acidic property of zirconia powder results in more rejection to CO<sub>2</sub>. The lower H<sub>2</sub>/CO<sub>2</sub> permselectivity of Zr-500 membrane can be assigned to the formation of mesoporous structures, though acid sites are still present in the membrane. Thus the acidic property plays a key role only if the membrane pore size is in the region of micropores.

### 3.4. Hydrothermal stability of microporous ZrO<sub>2</sub> membranes

The hydrothermal stability of microporous membranes is one of the most important properties for industrial gas separation, where hot steam is often encountered. In comparison with silica-based gas separation membranes, zirconia material is believed to be more stable in the presence of hot steam [20]. We have fabricated a sol-gel derived microporous zirconia membrane, with hydrogen permeance of  $5 \times 10^{-8}$  mol·m<sup>-2</sup>·s<sup>-1</sup>·Pa<sup>-1</sup> and H<sub>2</sub>/CO<sub>2</sub> permselectivity of 14. In this section, the stability of Zr-400 membrane in the presence of hot steam is studied. Fig. 7 shows H<sub>2</sub> and CO<sub>2</sub> permeances at 200 °C and calculated H<sub>2</sub>/CO<sub>2</sub> permselectivity as a function of exposure time to 100 kPa steam. After a small rise in the first 49 h exposure to steam, both H<sub>2</sub> and CO<sub>2</sub> permeances of Zr-400 membrane remain fairly constant at about  $4.7 \times 10^{-8}$  and  $3 \times 10^{-9}$  mol·m<sup>-2</sup>·s<sup>-1</sup>·Pa<sup>-1</sup>, respectively. The H<sub>2</sub>/CO<sub>2</sub> permselectivity is around 14 in this period, higher than the Knudsen value (4.7). Both H<sub>2</sub> and CO<sub>2</sub> permeances decrease after 400 h in-situ steam exposure, with the H<sub>2</sub> permeance decreasing to  $2.4 \times 10^{-8}$  mol·m<sup>-2</sup>·s<sup>-1</sup>·Pa<sup>-1</sup> and the CO<sub>2</sub> permeance reducing from  $3 \times 10^{-9}$  mol·m<sup>-2</sup>·s<sup>-1</sup>·Pa<sup>-1</sup> to  $9 \times 10^{-10}$  mol·m<sup>-2</sup>·s<sup>-1</sup>·Pa<sup>-1</sup> for the steam exposure time of 1250 h. Meanwhile, the H<sub>2</sub>/CO<sub>2</sub> permselectivity increased to a value of 27.4. The result can be ascribed to the viscous flow sintering of the membrane structure, which is promoted by the hot steam [34,35].

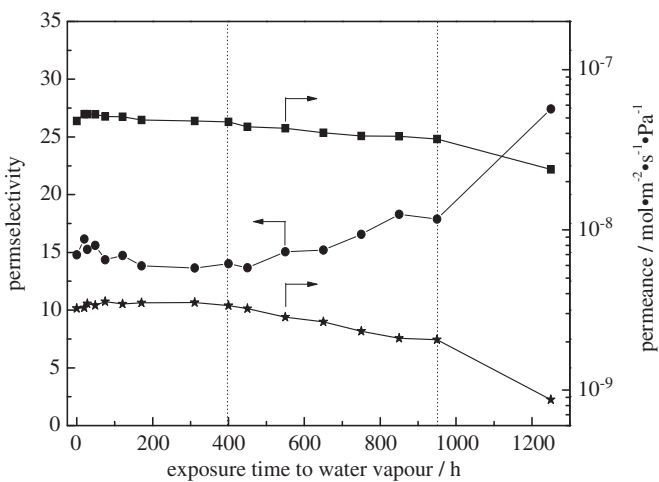


Fig. 7. Hydrothermal stability test of Zr-400 membrane, with H<sub>2</sub> and CO<sub>2</sub> gas permeances at 200 °C and calculated H<sub>2</sub>/CO<sub>2</sub> permselectivity as a function of exposure time to 100 kPa steam. ● H<sub>2</sub>/CO<sub>2</sub> permselectivity; ■ H<sub>2</sub> permeance; ★ CO<sub>2</sub> permeance.

To explain the variation of single gas permeance of sol-gel derived zirconia membranes, the properties of corresponding unsupported membrane (powder) were determined before and after steam treated in an autoclave, with the results displayed in Figs. 8 to 10. Fig. 8 shows

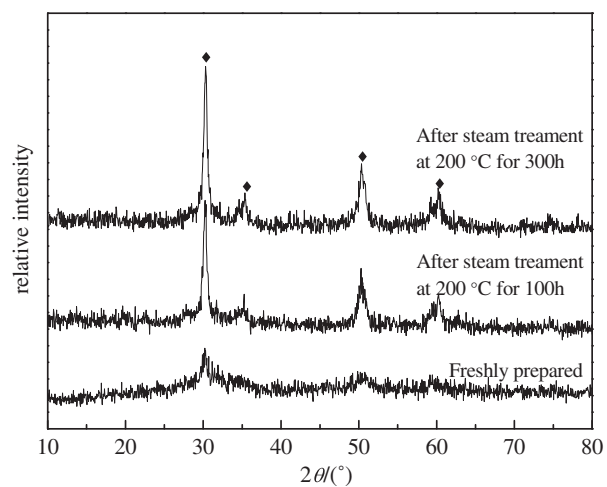


Fig. 8. XRD patterns of unsupported ZrO<sub>2</sub> membrane (powder) heat-treated at 400 °C before and after steam treatment. ♦ tetragonal.

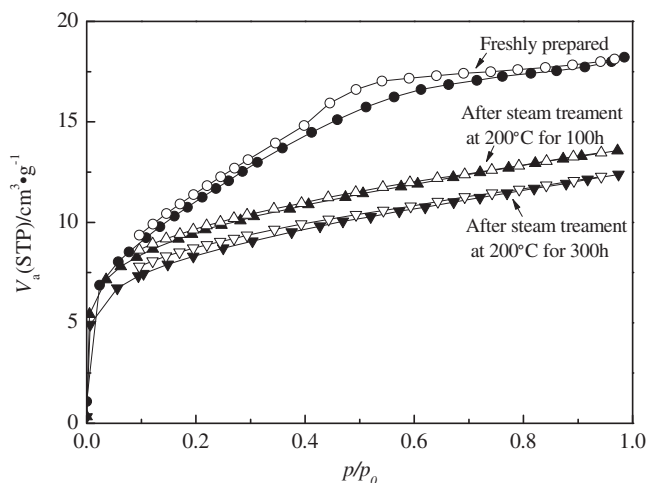


Fig. 9. Nitrogen adsorption/desorption isothermal curves of ZrO<sub>2</sub> powder heat-treated at 400 °C before and after steam treatment.

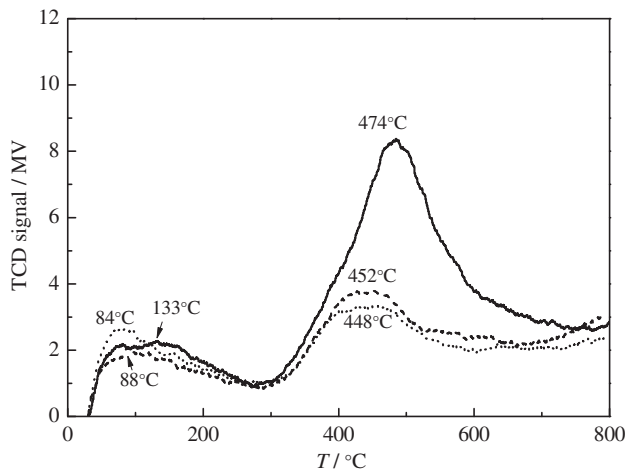


Fig. 10. NH<sub>3</sub>-TPD spectrogram of ZrO<sub>2</sub> powder heat-treated at 400 °C before and after steam treatment. — freshly prepared; - - - after steam treatment at 200 °C for 100 h; ..... after steam treatment at 200 °C for 300 h.

XRD patterns of Zr-400 powder before and after steam treatment for 100 and 300 h. In comparison with 400 °C-calcined zirconia powder, similar diffraction peaks can be observed. However, the powder with steam treatment exhibits more pronounced peaks of tetragonal phase, indicating the formation of more crystallized membrane structures with the exposure to hot steam. Coarse membrane crystalline structure, however, does not increase the membrane pore size, as evidenced by the nitrogen sorption data of zirconia powder displayed in Fig. 9. After 1550 kPa steam treatment for 100 and 300 h, both adsorption isotherm curves of zirconia powder show type I characteristics, indicating that the powder retains microporous structures during steam treatment. The results also confirm that part of the mesoporous structure inside the Zr-400 powder transforms to microporous one after exposure to steam. Additionally, the decrease in BET surfaces of zirconia powder after steam treatment indicates the partial densification of powder and prolonged exposure to hot steam will more or less accelerate the densification process. To ensure whether the acid sites in zirconia membrane play a key role in CO<sub>2</sub> transportation after steam treatment, NH<sub>3</sub>-TPD technique is used to determine the acid strength of Zr-400 powder before and after steam treatment, as shown in Fig. 10. In comparison with freshly prepared Zr-400 powder, both NH<sub>3</sub>-TPD curves of the powder exposed to steam for 100 and 300 h exhibit two distinct acid sites, corresponding to weak and moderate Lewis acids. Longer exposure to hot steam reduces the acid strength of zirconia powder, decreasing the ammonia desorption temperature. For example, with the powder treated by steam at 1550 kPa for 100 h, weak and moderate acid sites in zirconia powder shift from 133 °C and 474 °C to 88 °C and 452 °C respectively. The same tendency can be observed for the powder exposed to hot steam for 300 h. The reduction for intensity of corresponding peaks is another evidence, indicating the formation of weaker acidity in the powder. Thus the temperature of and the total area under NH<sub>3</sub>-TPD peaks, associated with acid strength and total number of acidic sites, respectively, decrease with the extension of steam treatment time. However, taken into account the nitrogen adsorption/desorption data in Fig. 9, it cannot be excluded that the densification of zirconia powder may be responsible for the lower adsorption capacity of ammonia (as shown in Fig. 10). From the single gas permeance of Zr-400 membrane exposed to hot steam (Fig. 7) and corresponding powder results (Figs. 8–10), we can conclude that it is densification rather than Lewis acid sites in the membrane plays a dominant role in imparting gas separation properties to zirconia membrane during exposure to hot steam. By comparison with published data (Table 2), the zirconia membrane in this study exhibits much higher hydrothermal stability.

**Table 2**  
Comparison of hydrothermal stability of ZrO<sub>2</sub> membranes with that of other microporous membranes in references

Membrane materials	Test temperature/°C	Steam pressure/kPa	Stability time/h	References
SiO <sub>2</sub>	200	12	220	[10]
Hybrid SiO <sub>2</sub>	300	300	90	[36]
Ni-SiO <sub>2</sub>	450	90	150	[8]
Co-SiO <sub>2</sub>	500	300	50	[37]
Nb-hybrid SiO <sub>2</sub>	200	100	311	[19]
ZrO <sub>2</sub>	200	100	1250	This work

#### 4. Conclusions

Microporous zirconia membranes with good H<sub>2</sub>/CO<sub>2</sub> permselectivity and excellent hydrothermal stability were fabricated via sol-gel process. The acidic sites in the membrane and microporous pores impart good H<sub>2</sub>/CO<sub>2</sub> permselectivity to the membrane. Mainly microporous

structures form in zirconia membranes calcined at 350 °C and 400 °C, with H<sub>2</sub> permeance of  $5 \times 10^{-8}$  mol·m<sup>-2</sup>·s<sup>-1</sup>·Pa<sup>-1</sup> and H<sub>2</sub>/CO<sub>2</sub> permselectivity of 14. Higher calcination temperature, 500 °C, results in the formation of mesoporous membrane.

Zirconia membrane calcined at 400 °C was chosen to investigate its stability in the presence of hot steam. After a small rise during the first 49 h exposure to 100 kPa steam, both H<sub>2</sub> and CO<sub>2</sub> permeances remained fairly constant. The H<sub>2</sub>/CO<sub>2</sub> permselectivity was maintained at around 14. Both H<sub>2</sub> and CO<sub>2</sub> permeances decreased after 400 h in-situ steam exposure, with H<sub>2</sub> and CO<sub>2</sub> permeances decreasing to  $2.4 \times 10^{-8}$  and  $9 \times 10^{-10}$  mol·m<sup>-2</sup>·s<sup>-1</sup>·Pa<sup>-1</sup>, respectively, for exposure of 1250 h to 100 kPa steam, while H<sub>2</sub>/CO<sub>2</sub> permselectivity increasing to 27.4. The results can be ascribed to viscous flow sintering of membrane, which is promoted by the hot steam, leading to densified membrane structures. The results indicate that sol-gel derived zirconia membranes may find potential use in gas separation processes.

#### References

- [1] N.W. Ockwig, T.M. Nenoff, Membranes for hydrogen separation, *Chem. Rev.* 107 (2007) 4078–4110.
- [2] G.Q. Lu, J.C. Diniz da Costa, M. Duke, S. Giessler, R. Socolow, R.H. Williams, T. Kreutz, Inorganic membranes for hydrogen production and purification: a critical review and perspective, *J. Colloid Interface Sci.* 314 (2007) 589–603.
- [3] S.N. Liu, G.P. Liu, W. Wei, F.J. XiangLi, W.Q. Jin, Ceramic supported PDMS and PEGDA composite membranes for CO<sub>2</sub> separation, *Chin. J. Chem. Eng.* 21 (2013) 348–356.
- [4] G.I. Spijksma, C. Huiskes, N.E. Benes, H. Kruidhof, D.H.A. Blank, V.G. Kessler, H.J.M. Bouwmeester, Microporous zirconia-titania composite membranes derived from diethanolamine-modified precursors, *Adv. Mater.* 18 (2006) 2165–2168.
- [5] H. Qi, Preparation of composite microporous silica membranes using TEOS and 1,2-bis(triethoxysilyl)ethane as precursors for gas separation, *Chin. J. Chem. Eng.* 19 (2011) 404–409.
- [6] H.L. Castricum, A. Sah, R. Kreiter, D.H.A. Blank, J.F. Ventec, J.E. ten Elshof, Hybrid ceramic nanosieves: stabilizing nanopores with organic links, *Chem. Commun.* (2008) 1103–1105.
- [7] R. Igi, T. Yoshioka, Y.H. Ikuhara, Y. Iwamoto, T. Tsuru, Characterization of co-doped silica for improved hydrothermal stability and application to hydrogen separation membranes at high temperatures, *J. Am. Ceram. Soc.* 91 (2008) 2975–2981.
- [8] M. Kanezashi, M. Asaeda, Hydrogen permeation characteristics and stability of Ni-doped silica membranes in steam at high temperature, *J. Membr. Sci.* 271 (2006) 86–93.
- [9] G.P. Fotou, Y.S. Lin, S.E. Pratsinis, Hydrothermal stability of pure and modified microporous silica membranes, *J. Mater. Sci.* 30 (1995) 2803–2808.
- [10] Q. Wei, F. Wang, Z.R. Nie, C.L. Song, Y.L. Wang, Q.Y. Li, Highly hydrothermally stable microporous silica membranes for hydrogen separation, *J. Phys. Chem. B* 112 (2008) 9354–9359.
- [11] M.C. Duke, J.C. Diniz da Costa, D.D. Do, P.G. Gray, G.Q. Lu, Hydrothermally robust molecular sieve silica for wet gas separation, *Adv. Funct. Mater.* 16 (2006) 1215–1220.
- [12] M.C. Duke, J.C. Diniz da Costa, G.Q. Lu, M. Petch, P. Gray, Carbonised template molecular sieve silica membranes in fuel processing systems: permeation, hydrostability and regeneration, *J. Membr. Sci.* 241 (2004) 325–333.
- [13] R.M. de Vos, W.F. Maier, H. Verweij, Hydrophobic silica membranes for gas separation, *J. Membr. Sci.* 158 (1999) 277–288.
- [14] M. Kanezashi, M. Sano, T. Yoshioka, T. Tsuru, Extremely thin Pd-silica mixed-matrix membranes with nano-dispersion for improved hydrogen permeability, *Chem. Commun.* 46 (2010) 6171–6173.
- [15] F. Shiba, B.H. Jeong, Y. Hasegawa, K.I. Sotowa, K. Kusakabe, Gas permeation through metal-loaded yttrium doped zirconia membranes, *Sep. Sci. Technol.* 39 (2004) 1259–1265.
- [16] Y.F. Gu, B.H. Jeong, K.I. Sotowa, K. Kusakabe, The effect of humidity on the durability of inorganic membranes, *J. Chem. Eng.* 20 (2003) 1079–1084.
- [17] C.C. Coterillo, T. Yokoo, T. Yoshioka, T. Tsuru, M. Asaeda, Synthesis and characterization of microporous ZrO<sub>2</sub> membranes for gas permeation at 200 °C, *Sep. Sci. Technol.* 46 (2011) 1224–1230.
- [18] R. Kreiter, M.D.A. Rietkerk, B.C. Bonekamp, H.M. van Veen, V.G. Kessler, J.F. Vente, Sol-gel routes for microporous zirconia and titania membranes, *J. Sol-Gel Sci. Technol.* 48 (2008) 203–211.
- [19] H. Qi, J. Han, N.P. Xu, H.J.M. Bouwmeester, Hybrid organic-inorganic microporous membranes with high hydrothermal stability for the separation of carbon dioxide, *ChemSusChem* 3 (2010) 1375–1378.
- [20] R. Vacassy, C. Guizard, V. Thoraval, L. Cot, Synthesis and characterization of microporous zirconia powders: application in nanofilters and nanofiltration characteristics, *J. Membr. Sci.* 132 (1997) 109–118.
- [21] G. Štefaníć, I.I. Štefaníć, S. Musić, Influence of the synthesis conditions on the properties of hydrous zirconia and the stability of low-temperature t-ZrO<sub>2</sub>, *Mater. Chem. Phys.* 65 (2000) 197–207.
- [22] J.P. Zhao, W.H. Fan, D. Wu, Y.H. Sun, Synthesis of highly stabilized zirconia sols from zirconium n-propoxide-diglycol system, *J. Non-Cryst. Solids* 261 (2000) 15–20.
- [23] L. Shi, K.C. Tin, N.B. Wong, Thermal stability of zirconia membranes, *J. Mater. Sci.* 34 (1999) 3367–3374.

- [24] G.I. Spijksma, D.H.A. Blank, H.J.M. Bouwmeester, V.G. Kessler, Modification of different zirconium propoxide precursors by diethanolamine. Is there a shelf stability issue for sol-gel applications? *Int. J. Mol. Sci.* 10 (2009) 4977–4989.
- [25] N. Agoudjil, S. Kermadi, A. Larbot, Synthesis of inorganic membrane by sol-gel process, *Desalination* 223 (2008) 417–424.
- [26] C.L. Chen, T. Li, S. Cheng, N.P. Xu, C.Y. Mou, Catalytic behavior of alumina-promoted sulfated zirconia supported on mesoporous silica in butane isomerization, *Catal. Lett.* 78 (2002) 1–4.
- [27] C.L. Shao, H.Y. Guan, Y.C. Liu, J. Gong, N. Yu, X.H. Yang, A novel method for making ZrO<sub>2</sub> nanofibres via an electrospinning technique, *J. Cryst. Growth* 267 (2004) 380–384.
- [28] K.S.W. Sing, D.H. Everett, R.A.W. Haul, L. Moscou, R.A. Pierotti, J. Rouquérol, T. Siemieniewska, Reporting physisorption data for gas/solid systems—with special reference to the determination of surface area and porosity (recommendations 1984), *Pure Appl. Chem.* 57 (1985) 603–619.
- [29] A. Díaz-Parralejo, A. Macías-García, E.M. Cuerda-Correa, R. Caruso, Influence of the type of solvent on the textural evolution of yttria stabilized zirconia powders obtained by the sol-gel method: characterization and study of the fractal dimension, *J. Non-Cryst. Solids* 351 (2005) 2115–2121.
- [30] M.E. Manríquez, T. López, R. Gómez, J. Navarrete, Preparation of TiO<sub>2</sub>–ZrO<sub>2</sub> mixed oxides with controlled acid-basic properties, *J. Mol. Catal. A Chem.* 220 (2004) 229–237.
- [31] W.H. Chen, H.H. Ko, A. Sakthivel, S.J. Huang, S.H. Liu, A.Y. Lo, T.C. Tsai, S.B. Liu, A solid-state NMR, FT-IR and TPD study on acid properties of sulfated and metal-promoted zirconia: influence of promoter and sulfation treatment, *Catal. Today* 116 (2006) 111–120.
- [32] H. Zou, Y.S. Lin, Structural and surface chemical properties of sol-gel derived TiO<sub>2</sub>–ZrO<sub>2</sub> oxides, *Appl. Catal. A Gen.* 265 (2004) 35–42.
- [33] D. Das, H.K. Mishra, A.K. Dalai, K.M. Parida, Isopropylation of benzene over sulfated ZrO<sub>2</sub>–TiO<sub>2</sub> mixed-oxide catalyst, *Appl. Catal. A Gen.* 243 (2003) 271–284.
- [34] Y.F. Gu, P. Hacarlioglu, S.T. Oyama, Hydrothermally stable silica-alumina composite membranes for hydrogen separation, *J. Membr. Sci.* 310 (2008) 28–37.
- [35] H. Imai, H. Morimoto, A. Tominaga, H. Hirashima, Structural changes in sol-gel derived SiO<sub>2</sub> and TiO<sub>2</sub> films by exposure to water vapor, *J. Sol-Gel Sci. Technol.* 10 (1997) 45–54.
- [36] M. Kanezashi, K. Yada, T. Yoshioka, T. Tsuru, Design of silica networks for development of highly permeable hydrogen separation membranes with hydrothermal stability, *J. Am. Chem. Soc.* 131 (2009) 414–415.
- [37] T. Tsuru, R. Igi, M. Kanezashi, T. Yoshioka, S. Fujisaki, Y. Iwamoto, Permeation properties of hydrogen and water vapor through porous silica membranes at high temperatures, *AIChE J.* 57 (2011) 618–629.